T2R2 東京科学大学 リサーチリポジトリ
Science Tokyo Research Repository

論文 / 著書情報
Article / Book Information

Title	EUV M3D parameter prediction of curvilinear mask patterns by convolutional neural networks
Authors	Moe Sugiyama, Masayuki Shimoda, Hiroyoshi Tanabe, Atsushi Takahashi
Citation	Proc. SPIE, Vol. 13980
Pub. date	2026, 2
DOI	https://doi.org/10.1117/12.3090321
Rights	(Copyright) Copyright 2026 Society of Photo-Optical Instrumentation Engineers (SPIE). One print or electronic copy may be made for personal use only. Systematic reproduction and distribution, duplication of any material in this publication for a fee or for commercial purposes, and modification of the contents of the publication are prohibited. (Citation) Moe Sugiyama, Masayuki Shimoda, Hiroyoshi Tanabe, and Atsushi Takahashi "EUV M3D parameter prediction of curvilinear mask patterns by convolutional neural networks", Proc. SPIE 13980, DTCO and Computational Patterning V, 139801J (10 April 2026); https://doi.org/10.1117/12.3090321
Note	This file is author (final) version.

Powered by T2R2 (Science Tokyo Research Repository)

EUV M3D Parameter Prediction of Curvilinear Mask Patterns by Convolutional Neural Networks

Moe Sugiyama, Masayuki Shimoda, Hiroyoshi Tanabe, and Atsushi Takahashi

Institute of Science Tokyo, Tokyo, Japan

ABSTRACT

Mask 3D (M3D) effects distort diffraction amplitudes from EUV masks. In our previous work, we developed a CNN that predicts M3D parameters very quickly from input mask patterns. M3D parameters enable us to reproduce distorted diffraction amplitudes from the mask. However, the mask patterns in the previous work are restricted to Manhattan patterns. Generally, the accuracy of neural networks depends on the training data. The CNN trained on Manhattan patterns could not be applied to other types of mask patterns. Recently, curvilinear mask patterns have become popular due to advancements in multibeam EB mask writers. Curvilinear patterns have advantages over Manhattan patterns regarding lithography process margins. In this work, we generate curvilinear mask patterns by using ILT technique in order to utilize them as training data to obtain a more comprehensive CNN for M3D parameter prediction. The performance of the CNN trained with/without curvilinear patterns is discussed.

Keywords: Neural networks, Mask 3D effects, EUV, Curvilinear pattern

1. INTRODUCTION

Lithography is one of the most critical steps in semiconductor manufacturing. Achieving a high yield and performance requires the optimization of the lithography process, including source shapes and mask patterns.[1] Lithography simulation is essential for optimizing and evaluating the lithography process.

In extreme ultraviolet (EUV) lithography, high aspect ratio absorbers used in EUV masks (Fig. 1) induce several mask three-dimensional (M3D) effects that cause critical dimension and image placement errors.[2,3] Conventional lithography simulations treat light as a scalar wave and compute the light intensity on the wafer. However, such scalar approximations cannot accurately model the M3D effects. Since photoresist materials primarily respond to the electric field of light, accurate prediction of wafer patterns requires precise computation of the electromagnetic field while accounting for the M3D effects. This necessitates electromagnetic (EM) simulations, which are known to be computationally expensive.

To mitigate this cost, we proposed CNN-based methods that predict M3D parameters from mask patterns (Fig. 2), thereby replacing full EM simulations.[4] By using the predicted M3D parameters, wafer patterns can be computed with an accuracy comparable to EM simulations (Fig. 3) while achieving approximately $3,000\times$ speedup. The ultimate goal of our study is to construct a CNN that can accurately infer M3D parameters for arbitrary mask patterns used in the industry.

Conventional masks have mainly employed Manhattan patterns due to manufacturing constraints. In our previous study, we also used Manhattan patterns as the training data for the CNN. Recently, multi-beam mask writing technology has been introduced for EUV mask fabrication,[5] enabling the direct writing of curvilinear patterns without increasing mask writing time. The pattern fidelity and process margin on the wafer are improved by using curvilinear mask patterns. This advancement promotes the adoption of curvilinear masks in practical manufacturing.

Our CNN-based M3D parameter prediction methods used only Manhattan patterns as training data. Manhattan patterns are generated by randomly sampling pattern parameters such as linewidth, line length, and

Further author information: tanabe@eda.ict.eng.isct.ac.jp

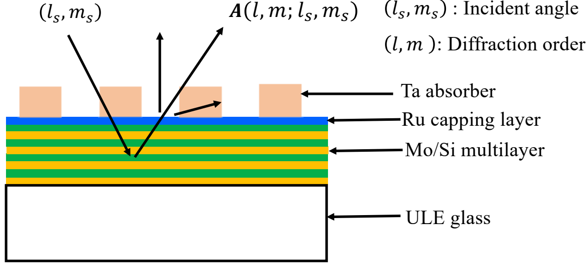

Figure 1: EUV mask.

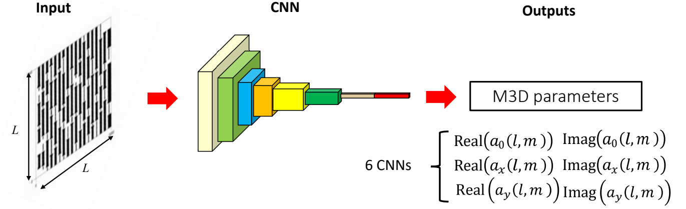

Figure 2: CNN inference for M3D parameters.

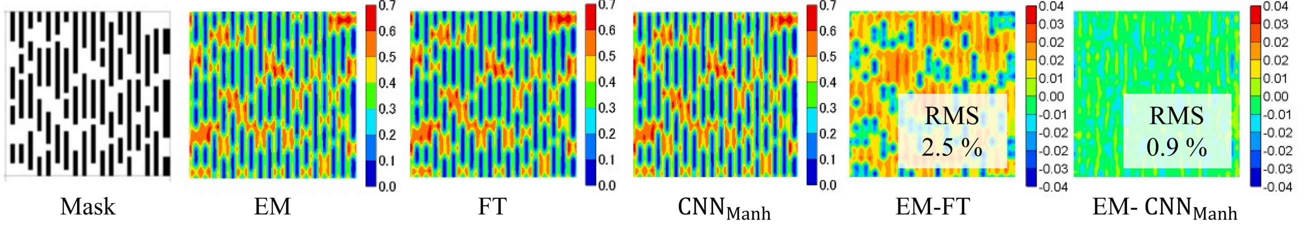

Figure 3: Image intensities on Manhattan pattern.[4]

spacing derived from practical mask designs. As a result, while high accuracy is achieved for Manhattan patterns, prediction accuracy degrades for curvilinear patterns. Therefore, a CNN capable of accurately predicting M3D parameters for curvilinear patterns is required.

In this study, we aim to develop a CNN capable of predicting M3D parameters for practical curvilinear patterns. As a first step, the CNN is trained with a dataset of curvilinear VIA patterns. The curvilinear patterns are generated using OpenILT,[6] replacing the optical kernels with EUV kernels. The experimental results demonstrate that, with a sufficiently large training dataset, M3D parameters can be predicted with high accuracy for curvilinear VIA patterns.

2. CONVOLUTIONAL NEURAL NETWORKS FOR M3D PARAMETERS

In conventional optical lithography simulations, the light-shielding film of a mask is assumed to be very thin. Under this assumption, the far-field diffraction amplitude is calculated by the Fourier transformation (FT) of the mask pattern, and the amplitude is independent of the incident angle (or source position). In contrast, in EUV lithography simulations, since the aspect ratio of the absorber is high, the far-field diffraction amplitude $\boldsymbol{A}(l, m; l_s, m_s)$ (vector potential) is calculated by the EM simulation, where (l, m) represents the diffraction order and (l_s, m_s) represents the source position. In this case, the amplitude depends on both the diffraction order and the source position, as shown in Fig. 1.

Following our previous work, the thick mask diffraction amplitude $\boldsymbol{A}(l, m; l_s, m_s)$ is decomposed into the thin mask amplitude $\boldsymbol{A}^{\mathrm{FT}}(l, m)$, which is obtained by the FT of the mask pattern, and the residual M3D amplitude $\boldsymbol{A}^{\mathrm{3D}}(l, m; l_s, m_s)$, as follows.

$$\boldsymbol{A}(l, m; l_s, m_s) = \boldsymbol{A}^{\mathrm{FT}}(l, m) + \boldsymbol{A}^{\mathrm{3D}}(l, m; l_s, m_s).$$

Thin mask amplitude $\boldsymbol{A}^{\mathrm{FT}}$ can be obtained very quickly by FT and constitutes the dominant component of the total diffraction amplitude $\boldsymbol{A}$. The contribution of the M3D amplitude $\boldsymbol{A}^{\mathrm{3D}}$ is relatively small but not negligible. It varies smoothly with the incident angle (l_s, m_s). This angular dependence is approximated by a linear function of l_s and m_s, as follows:[4]

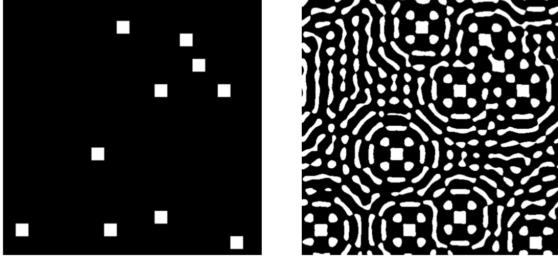

(a) Target pattern. (b) Output mask.

Figure 4: Curvilinear pattern generation by OpenILT.

Table 1: Generated datasets.

dataset	#total		#original	
type	train	val	train	val
small	5,000	20	100	20
medium	50,000	200	1,000	200
large	500,000	1,000	10,000	1,000

$$A_x^{3D}(l,m;l_s,m_s) \simeq a_0(l,m) + a_x(l,m)\left(l_s + \frac{l}{2}\right) + a_y(l,m)\left(m_s + \frac{m}{2}\right).$$

Constant $a_0(l,m)$ and coefficients $a_x(l,m)$ and $a_y(l,m)$ are called M3D parameters. M3D parameters are the key metrics of the M3D effect, and these parameters are determined by the mask pattern.

A CNN that predicts M3D parameters from an input mask pattern is shown in Fig. 2. In the implementation, six CNNs are used depending on the targets: $\mathrm{Real}(a_0(l,m))$, $\mathrm{Imag}(a_0(l,m))$, $\mathrm{Real}(a_x(l,m))$, $\mathrm{Imag}(a_x(l,m))$, $\mathrm{Real}(a_y(l,m))$, and $\mathrm{Imag}(a_y(l,m))$. There are about 1,900 (l,m) pairs for a 2,048 nm X 2,048 nm mask clip when NA = 0.33. The accuracy of the CNN depends on the training dataset. In the next section, methods of dataset preparation are discussed.

3. DATASET PREPARATION FOR CNN TRAINING

3.1 CURVILINEAR MASK PATTERN

A mask generated for training data is a dark-field mask with the size of (H, W) = (2,048, 2,048), where each pixel corresponds to a nanometer-scale physical dimension. The target pattern of each mask contains 10 to 15 VIAs (vertical interconnect accesses). The corresponding M3D parameters, which serve as the label data, are obtained by EUV simulations based on our previous work.[4]

The VIAs in a target pattern are randomly generated one by one without overlap. Each VIA has a size of 100 nm $\times$ 100 nm. VIA locations are restricted to grid points with a pitch of 100 nm, resulting in 400 candidate placement points within the target region. To prevent physical contact between adjacent VIAs, once a VIA is generated on a grid point, the eight neighboring grid points are excluded from subsequent location candidates. This constraint ensures that all VIAs are spatially isolated from each other.

After generating the target VIA patterns, curvilinear mask patterns are obtained from the target VIA patterns using OpenILT,[6] as shown in Fig. 4. In this study, CurvILT in OpenILT,[6] which is based on MOSAIC,[7] is used as the ILT algorithm, and its kernels are replaced from optical kernels to EUV kernels. In the lithography simulations, a conventional illumination source is assumed. The exposure conditions are set to a numerical aperture of NA = 0.33, a coherence factor of $\sigma = 0.6$, and a wavelength of $\lambda = 13.5$ nm.

3.2 DATA AUGMENTATION

Deep neural networks generally require a large amount of training data to achieve high accuracy. However, the variability of the randomly generated mask patterns described in the previous section is inherently limited. To address this issue, the effective size of the training dataset is increased by applying data augmentation techniques.

Various data augmentation methods have been proposed in the literature. In this study, the training dataset is expanded using shift-based augmentation, following existing work.[8] Specifically, new training samples are generated by shifting the original VIA mask patterns by displacements Δx and Δy. Circular padding is used because the M3D parameters of the shifted mask pattern can be easily calculated by multiplying a phase factor caused by the FT, under the periodic boundary condition. The values of Δx and Δy are randomly generated according to a uniform distribution within the range $[0, 512)$.

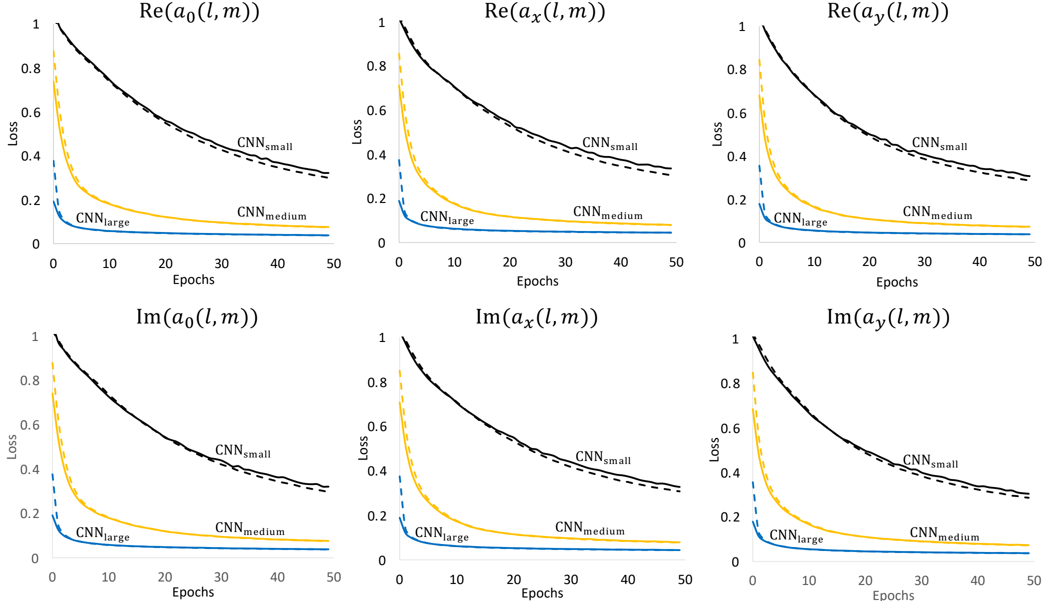

Figure 5: Loss curve with three benchmarks. The dashed line represents the training loss, while the solid line represents the validation loss.

3.3 CNN ACCURACY

To investigate how the CNN accuracy varies with the size of the dataset, three datasets, namely small, medium, and large, are prepared, as summarized in Table 1. In Table 1, "#total" denotes the total number of samples used for training and validation, whereas "#original" indicates the number of samples generated without data augmentation among those samples. For the small dataset, 100 VIA mask patterns are randomly generated using the method described above, and the dataset is expanded to 5,000 samples through data augmentation, corresponding to a 50-fold increase in the number of samples. The same 50-fold data augmentation procedure is applied to the medium and large datasets.

CNN trained with small, medium, large datasets are called CNN$_{\mathrm{small}}$, CNN$_{\mathrm{medium}}$, and CNN$_{\mathrm{large}}$, respectively. The CNN architecture is a VGG[9]-like network, which is the same as existing work.[8] For each dataset, CNN was trained for 50 epochs using Adam optimization algorithm,[10] with a learning rate set to 0.001.

Figure 5 shows the loss curves of the training and validation for each dataset. For all datasets, the difference between the training loss and the validation loss was small, indicating that the training was completed without overfitting. Furthermore, the loss decreased as the size of the training dataset increased.

4. IMAGE INTENSITY COMPARISON

Figure 6 shows a comparison of the image intensities obtained by the CNNs trained on each dataset and those obtained by EM simulations. As an evaluation metric, the difference between the corresponding optical intensity distributions was calculated, and the maximum value, minimum value, and range of the differences were compared. The intensity difference between the EM simulation and CNN$_{\mathrm{small}}$ was 3.8% (maximum 1.8%, minimum −1.9%). In contrast, the difference between the intensities obtained by the EM simulation and CNN$_{\mathrm{large}}$ was reduced to 1.7% (maximum 1.4%, minimum −0.3%), demonstrating a significant improvement in accuracy.

Next, simulation accuracy using the CNN trained with the large dataset CNN$_{\mathrm{large}}$ is compared with those of the thin mask model using the Fourier transform (FT) of the mask pattern and the CNN model trained with the Manhattan pattern dataset CNN$_{\mathrm{Manh}}$. Figure 7 shows the intensity comparison results. The difference in image intensity was 8.7% (maximum 4.9%, minimum −3.8%) between the EM and FT results, the difference between the EM and CNN$_{\mathrm{Manh}}$ was 6.0% (maximum 2.4%, minimum −4.6%), while the difference between the EM and

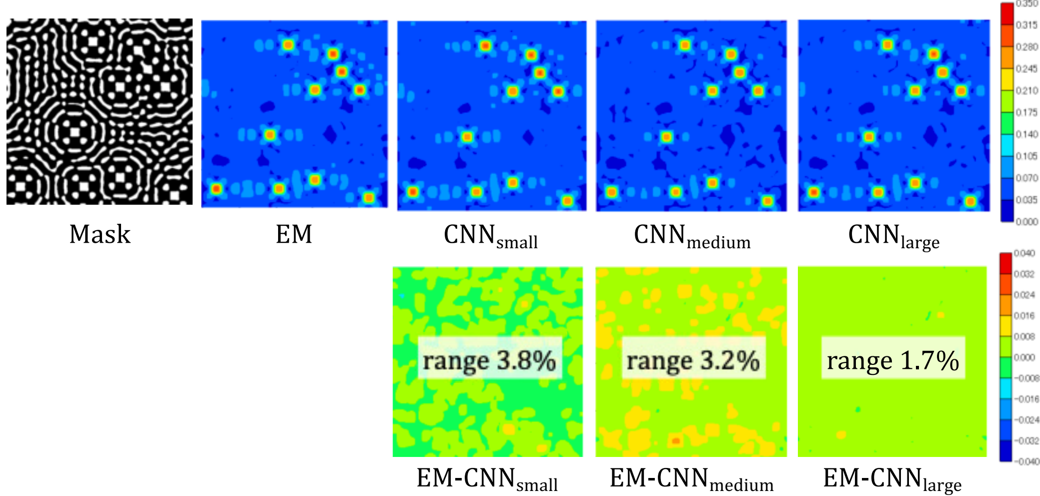

Figure 6: Image intensity calculated with CNNs trained by various amount of data.

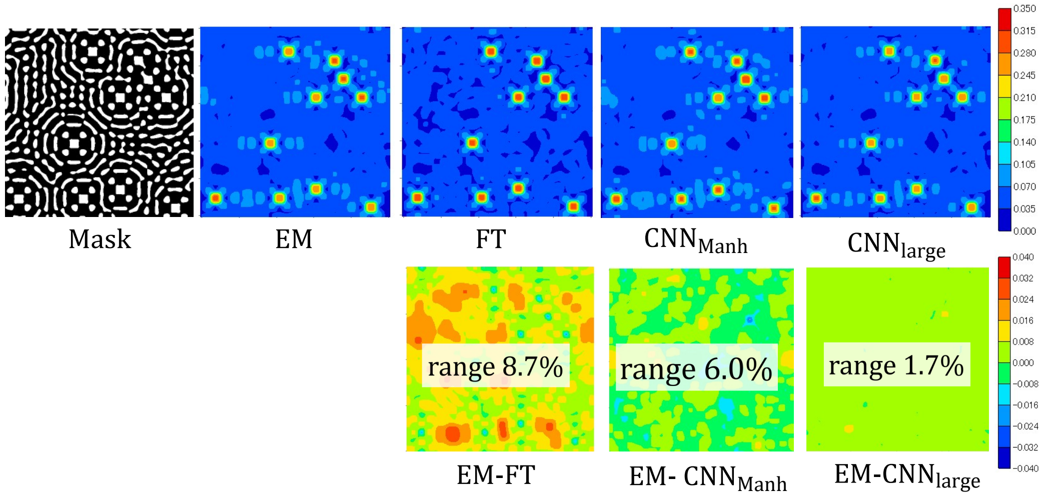

Figure 7: Image intensity comparison.

$\mathrm{CNN}_{\mathrm{large}}$ was only 1.7% (maximum 1.4%, minimum −0.3%), demonstrating that our approach significantly improves simulation accuracy.

In the EUV simulation formulation assumed in this study, the M3D parameters are defined to depend only on the mask pattern. Therefore, the proposed method is applicable under various defocus conditions required in practical use. Figure 8 shows the simulated intensity results for defocus values of ±50 nm and ±100 nm. The results demonstrate that the CNN-based simulation accurately calculates the intensity under different defocus conditions.

5. SUMMARY

In this paper, CNNs were employed to infer M3D parameters from curvilinear mask patterns. The curvilinear mask patterns were generated using OpenILT, and the training datasets were expanded through data augmentation. Experimental results demonstrate that increasing the dataset size reduces the validation loss and improves the inference accuracy of the M3D parameters.

These results suggest that a CNN is capable of inferring M3D parameters for curvilinear mask patterns. In future work, we will evaluate the inference accuracy with a broader range of pattern types and aim to realize a highly accurate CNN applicable to arbitrary mask patterns used in the industry.

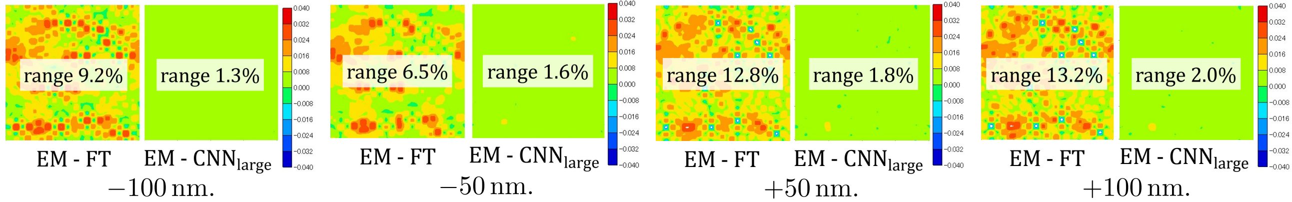

Figure 8: Intensity with various defocus settings.

ACKNOWLEDGMENTS

This work was partially supported by JSPS KAKENHI Grant Number JP25K03090, MEXT Initiative to Establish Next-generation Novel Integrated Circuits Centers (X-NICS) Grant Number JPJ011438, and Japan Science and Technology Agency (JST) as part of Adopting Sustainable Partnerships for Innovative Research Ecosystem (ASPIRE), Grant Number JPMJAP2514.This study was carried out using the TSUBAME4.0 supercomputer at Institute of Science Tokyo.

REFERENCES

[1] Wong, A. K., [*Resolution enhancement techniques in optical lithography*], SPIE press (2001).

[2] Philipsen, V., "Mask is key to unlock full euvl potential," in [*Extreme Ultraviolet (EUV) Lithography XII*], **11609**, 1160904, SPIE (2021).

[3] Erdmann, A., Evanschitzky, P., Bottiglieri, G., van Setten, E., and Fliervoet, T., "3d mask effects in high na euv imaging," in [*Extreme Ultraviolet (EUV) Lithography X*], **10957**, 219–231, SPIE (2019).

[4] Tanabe, H., Shimoda, M., and Takahashi, A., "Rigorous electromagnetic simulator for extreme ultraviolet lithography and convolutional neural network reproducing electromagnetic simulations," *Journal of Micro/Nanopatterning, Materials, and Metrology (JM3)* **24**(2), 024201–1–024201–17 (2025). doi:10.1117/1.JMM.24.2.024201.

[5] Matsumoto, H., Yasuda, J., Motosugi, T., Kimura, H., Kawaguchi, M., Kojima, Y., Yamashita, H., Saito, M., Tamura, T., and Nakayamada, N., "Multi-beam mask writer mbm-3000 for next generation euv mask production," in [*Photomask Technology 2023*], **12751**, 263–269, SPIE (2023).

[6] Zheng, S., Ma, Y., Zhu, B., Chen, G., Zhao, W., Yin, S., Yu, Z., and Yu, B., "OpenILT: An open-source platform for inverse lithography technique research." https://github.com/OpenOPC/OpenILT/ (2023).

[7] Gao, J.-R., Xu, X., Yu, B., and Pan, D. Z., "Mosaic: Mask optimizing solution with process window aware inverse correction," in [*Proceedings of the 51st Annual Design Automation Conference*], *DAC '14*, 1–6, Association for Computing Machinery, New York, NY, USA (2014).

[8] Tanabe, H. and Takahashi, A., "Data augmentation in extreme ultraviolet lithography simulation using convolutional neural network," *Journal of Micro/Nanopatterning, Materials and Metrology (JM3)* **21**(4), 041602–1–041602–10 (2022). doi:10.1117/1.JMM.21.4.041602.

[9] Simonyan, K. and Zisserman, A., "Very deep convolutional networks for large-scale image recognition," *arXiv preprint arXiv:1409.1556* (2014).

[10] Kingma, D. P., "Adam: A method for stochastic optimization," *arXiv preprint arXiv:1412.6980* (2014).